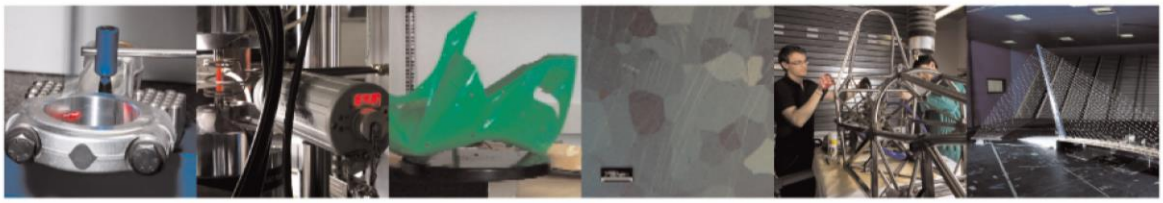

Model-based adaptive process control for surface finish improvement in traverse grinding

Parenti, Paolo; Leonesio, Marco; Bianchi, Giacomo

This is a post-peer-review, pre-copyedit version of an article published in MECHATRONICS.
The final authenticated version is available online at:
http://dx.doi.org/10.1016/j.mechatronics.2016.04.001

DIPARTIMENTO DI MECCANICA ■ POLITECNICO DI MILANO
via G. La Masa, 1 ■ 20156 Milano ■ EMAIL (PEC): pecmecc@cert.polimi.it
http://www.mecc.polimi.it
Rev. 0

Model-based adaptive process control for surface finish improvement in traverse grinding

Paolo Parenti[1,*], Marco Leonesio[2], Giacomo Bianchi[2]

[1] Department of Mechanical Engineering, Politecnico di Milano, via La Masa 1, 20156, Milan, Italy

[2] CNR, Institute of Industrial Technology and Automation, via Bassini 15, 20133, Milan, Italy

*Corresponding author: paolo.parenti@polimi.it

Model-based adaptive process control for surface finish improvement in traverse grinding

Abstract

The paper presents a process controller aimed at improving the surface quality generated by traverse grinding, avoiding the surface defects caused by vibrations onset. The innovation provided by the proposed controller consists in suppressing vibration occurrence by means of a model-based and self-learning approach: a monitoring layer classifies occurring problems and a control logic exploits these indications to select the proper mitigation actions. Since wheel-regenerative chatter represents one of the most important problems during traverse grinding in terms of achievable productivity and finishing quality, the main control variable is the wheel velocity. This variable is tuned exploiting an adaptive Speed tuning Map computed by the controller using a heuristic approach and learning methodology. The control can manage also the other sources of vibration by means of proper identification and mitigation strategies. Experimental tests are carried out on a roll grinder to validate the control system. Good performances are achieved after some training tests to allow controller learning.

Keywords*:* Process Control; Traverse Grinding; Chatter marks; Waviness; Regenerative Vibration; State-machine.

NOMENCLATURE

h_0	Commanded infeed [mm]	X	Radial/Normal direction
$d_r(t)$	Relative displacement between wheel and workpiece centers [mm]	Y	Tangential direction
$h(t)$	Actual engaged infeed at time t [mm]	k_t	Grinding specific energy [N/mm^2]
$w(t)$	Radial wheel wear at time t [mm]	μ	Friction Ratio
G_r	Radial Grinding Ratio	$\ddot{X}_k$	Accelerometer readings [m/s^2]
G	Volumetric Grinding Ratio	w_k	Weights for sensors averaging
$Q_{s,w}$	Wheel and Workpiece material removal rate [mm^3/s]	N	Number of harmonics

b	Cutting width [mm]	$a_{S,}a_{W}$	Wheel and Workpiece complex waviness amplitude
$v_{s,w}$	Wheel and Workpiece tangential speed [m/s]	T	Sensor Transmissibility function
s	Laplace operator	$\Im$	Fourier transform
ω	Fourier operator		
k_c	Wheel rigidity [N/m]	n	Number of grinding passes in a cycle
τ, T_p	Time constants	α	Map update Weighting factor
$H(\omega)$	wheel-workpiece relative FRF	US_t	Updated wheel speed? score vector
OSM_t SSM_t FSM_t	Stability maps scores: Original, Smoothed, Filtered by operator preferences.	γ	Data aging Weighting factor
L,R	Open and Closed loop Transfer Function	Δe	Epoch time span
I	Identity Matrix	OS_t	Operator Map Score
P_{pos},P_{vel}	Cutting Process proportional and derivative coefficients matrices	β	Operator Weighting factor
$D_{s,w}$	Wheel and Workpiece diameter [mm]	L_T	Cylinder length
$\omega_{s,w}$	Wheel and Workpiece rotational speed [rad/s]	$\Delta h_{S,W}$	Radius deviations due to waviness
$\theta_{S,W}$	Wheel and Workpiece angular position [rad]	$\mathrm{H}_{\mathrm{NCL}}$	Radial closed-loop structural response

1. INTRODUCTION

The current manufacturing environment places a growing demand on autonomous control of manufacturing processes, especially in unattended machines. In grinding, operator surveillance is required to cope with the strong process variability introduced by the tool characteristics. One of these is the wear evolution that decreases the final quality of the machined products through different mechanisms, as the vibration that results in the production of marked workpieces. The produced defects, often called "chatter marks", represent the most important surface defect of cylindrical products, such as hot rolling rolls: a periodical surface waviness with pitches ranging up to tens of millimeters and with amplitudes ranging up to tens of microns. Whenever the system

vibrates, wheel and roll undergo a relative oscillation, mainly in the radial direction, modulating the actual infeed. Then, periodic surface defects are generated in the form of waviness on the workpiece and in some cases on the grinding wheel surface. The problem is very complex because different phenomena can lead to vibration onset and consequent waviness generation: wheel unbalance or roundness error, process instability due to modal coupling or surface regeneration (i.e. workpiece regenerative chatter and wheel regenerative chatter).

The presence of this defect on the machined rolls has to be avoided since it has detrimental effects either on the surface appearance of the cylinders (i.e. quality acceptance) and on their functionality in the rolling operations. In their paper, Panjkovic et al. [1] claimed that the presence of chatter marks in work rolls of rolling mills are also linked to vibration (both forced and self-induced) rising in the rolling plant.

In general, optimization strategies for grinding operations have been designed by many authors in literature. In their comprehensive review, Rowe et al. [2], show that most of them rely on Artificial Intelligence (AI). Among these techniques, two big families are identified consisting in desktop systems to assist tool and parameter selection and self-optimizing systems integrated within the machine controller. As stated by Chen and Tian [3], however, only few optimization algorithms in literature include an explicit term related to chatter instability in the optimization process, while dimensional accuracy is often the paramount objective. In fact, Choi and Lee [4] have developed an active control system for thermal error compensation in cylindrical grinding of long slender rolls. They have achieved a 30% improvement of workpiece cylindricity by means of actuated workpiece rests that cope with the quasi-static thermal machine distortion and the related variation of mechanical compliance. However, the very low bandwidth of the control system does not permit to address problems related with the dynamical compliance of the mechanical system.

Möhring et al. [5] have developed an active error compensation system, involving hydraulic and piezoelectric actuators, for the compensation of distortions and unequal allowance distributions in crankshafts grinding. Thanks to the developed model-based approach and the active 2-DOF tailstock, the system provides an accuracy improvement and a reduction of spark out time.

Hekman and Liang [6] presented a method for optimizing the part parallelism in surface grinding by adopting a real-time depth of cut manipulation based on the machine predicted deflection and on the use of a dynamometer installed on the machine. This work however addresses only geometrical errors of the part and does not consider the surface accuracy optimization of the ground components.

On the other side, Inasaki [7] designed a methodology to monitor and control grinding processes, by using AI and including chatter in plunge grinding and by exploiting Acoustic Emission (AE) and power sensors. The monitoring approach showed good

results however, it is not included in a real-time adaptive control of the grinding machine to produce an effective cutting process optimization.

Yuan et al. [8] tested in simulation the application of a fuzzy-logic controller (FLC) in roll grinding system, coping with the double regeneration problem. The control system showed good vibration reduction compared to a conventional control method. However, the feasibility and robustness of their approach on real applications has not been discussed.

Classical solutions based on active vibration suppression have also been studied for improving the accuracy on the parts: in this case, the main challenge consists in developing a measuring system able to perceive (or estimate) the micrometric displacements between wheel and workpiece, together with the proper actuating system that must be capable of influencing the system behavior.

Oh and Kim [9] developed an optical PID vibration control relying on an electromagnetic inertial actuator installed on a small grinder. Good system performance was shown on the laboratory test-rig, but no verifications in relevant industrial environments, with all the associated variables that could limit the actual system efficacy, were presented. Similarly, Albizuri at al. [10] adopted piezoelectric actuators, characterized by a high frequency bandwidth, in a small centerless grinding machine. The solution is effective but, due to the system dimensions, its applicability in other situations as the case of a large traverse grinding machine (such as the roll grinders) is limited. Nakano et al. [11] showed that passive vibration dampers can be properly adopted to cope with chatter issues, but they lack of automatic adaptivity. In this regard, it must be noted that large variability in close loop grinding machine dynamics may arise for several reasons. For instance, the cumulated wear of the grinding wheel affects cutting process coefficients and can cause a large change of the wheel mass affecting the modes of vibration of the spindle. Wear of machine components, such as spindle bearings or workpiece support pads, can also introduce variation on the machine dynamics. Similarly, variation of workpiece geometry and related weight could affect machine dynamics in terms of vibration mode shapes and frequencies. For these reasons, automatic adaptivity is considered as an important property for implementing effective process control at industrial scenarios level.

On the other side, regenerative chatter is a well-known phenomenon in many machining processes and is well investigated by Altintas and Weck [12] and other authors in the grinding literature. Several works have been dedicated to the analysis of process parameters effect on chatter onset. Inasaki et al. [13] presented a comprehensive survey, proposing models and chatter avoidance techniques. In that review, different mitigation and chatter control strategies are discussed, comprising modification of process parameters, as well-known in industrial practice. Indeed, a proper selection of grinding parameters may have a direct effect on the regeneration phenomenon improving cutting performance. This optimization, usually carried out by grinding experts during the first setup of a grinding cycle (in "out-of-process" phase), is mainly based on empirical knowledge and it depends on the

different working situations and machine characteristics. A pioneering attempt to exploit theoretical knowledge to carry out an "out-of-process" optimization has been undertaken by Thompson [14],[15]: it is based on wheel and workpiece regenerative chatter theory. Unfortunately, any change of the system dynamic behavior during machine operations (e.g. due to machine components wear) or wheel type or cutting condition requires the cutting parameters to be updated with new optimal values. Supporting this claim, several detailed studies have been published pointing out how grinding stability is influenced by several factors. Among them, Orynski and Pawlowski [16] claimed that cutting parameters are one of the most significant factors for chatter, in particular the wheel/workpiece speeds, the commanded infeed and the wheel width. Later, Li and Shin [17] developed a numerical solution for chatter stability that considers these parameters in plunge grinding; process condition-dependent dynamics is also taken into account in the study. The chatter reduction properties, provided by applying a continuous speed variation technique, have been recently discussed by Alvarez et al. [18], showing that, under certain circumstances, chatter can be properly mitigated by this technique. Pearce [19] studied, both theoretically and experimentally, the effect of the wheel dressing parameters (dresser position, wheel speed and workpiece regeneration) on the cutting instability; he showed that these factors play a key role in mitigating the regenerative chatter onset, with special emphasis on the improvements provided by the continuous dressing technique. Leonesio et al. [20] have demonstrated that structural mode shapes can induce a force-field cutting instability in grinding processes, thus confirming standard regenerative phenomenon is not the only reason inducing cutting instability. Mannan et al. [21] have studied the effect on chatter onset of the torsional compliance introduced by wheel spindle, considering a linearization of the system dynamics and then applying a frequency domain approach. With a similar modelling approach, Baylis and Stone [22] have evaluated the destabilizing effect introduced by the specific wheel flexibility, utilizing digital simulations to justify the very slow precession rates of wheel waves around the circumference of the wheel during the onset of regenerative chatter.

Moving from these premises, a novel chatter controller for cylindrical traverse grinding, in particular roll grinding, is presented in this paper. It merges the *a-priori* knowledge on the regenerative chatter phenomenon with the adaptiveness typical of AI strategies. The *a-priori* knowledge about regenerative chatter (mainly concerned with frequency contents and wheel lobing effect) allows the development of an algorithm for a fast chatter detection and identification of the proper control action. In literature several grinding monitoring algorithms, in particular for chatter identification, have been proposed in the last decades, as reviewed by Tönshoff et al. [23]. Among them, Fu et al. [24] presented one of the most interesting chatter monitoring approaches, based on the application of an entropy function and of a morphological filtering. They have developed a system able to perform the monitoring and identification of both wheel and workpiece regenerative chatter in the traverse grinding process by analyzing the vibration spectrum. Data analysis showed that the monitoring method was successful in different conditions but

the overall robustness, with respect to real-time industrial implementations on industrial control hardware, has not been tested, especially considering the computational lightness required for the deployment in an industrial control hardware. More recently, González-Brambila et al. [25] demonstrated that an effective indicator for grinding process monitoring is based on wavelet transform extracted from contact measurements of the final component. The method has proved to be satisfactory on production parts, but it has the major limitation of requiring off-line workpiece measurements that limits the overall system productivity. Based on the aforementioned review, it is clear that no specific adaptive control systems have been developed so far for mitigating the chatter onset and the resulting surface defects, in traverse grinding. This motivated the presented study that introduces an innovative model-based adaptive process controller for improving the workpiece surface finishing in industrial traverse grinding operations. The paper is structured as follows: first, the process controller architecture is presented, describing the modules devoted to monitoring, control and self-adaption. Implementation details are also provided for the reader. Then, the controller effectiveness is validated by means of experimental tests on a commercial roll grinder in a real industrial context. Finally, discussions and conclusions are presented, elaborating on the possibility of extending the current controller with other functionalities focused on a broader set of performance.

2. CONTROLLER OBJECTIVE AND ARCHITECTURE

The proposed controller aims at suppressing the effects of wheel/workpiece relative vibrations on workpiece surface. Avoiding the formation of undesired waviness (consequent to vibration onset) on cylinder surface represents the main control objective. The control variables are a subset of the classical technological parameters used in traverse grinding:

- Wheel angular velocity ($\boldsymbol{\omega}_s$)
- Cylinder velocity (V_w)
- Number of grinding passes (n)

Controller feedback relies on a set of signals coming from different sensors whose measurements, influenced by process vibration occurrence, can be exploited for monitoring vibrations in terms of level and origin via a sensor-fusion approach. In particular:

- Spindles current signals (both wheel and cylinder)
- Accelerometers (installed in sensitive positions on the machine structure)
- Additional sensors (e.g. Acoustic Emission-AE)

The controller is implemented following a state machine concept (details can be found in Sakarovitch [26]). The controller is characterized by an "open structure", that easily allows further development and improvements to the control logic, in adaptation

to varying operating conditions. “Intelligent” synthetic indicators, embedding knowledge about the process, trigger the transitions between states (Figure 1). In particular, indicators must provide a quantitative estimation of the generated waviness in real-time for triggering the proper control actions. A model-based waviness observer module, based on accelerometers installed in different points of the grinder, is exploited to produce this estimation relying on a process-machine dynamic model. The control actions are also governed by an additional set of heuristic rules derived from practical experience, to optimize the overall performance in real industrial environments. Moreover, the rules driving the selection of the best wheel velocity rely upon an evolving memory structure with self-learning adaptive capabilities.

The controller architecture is presented in the listed paragraphs:

- Vibration cause and related Chatter Indicator (par. 2.1 - 2.2)
- Observer of the formed waviness (par. 2.3)
- State machine integrating the control logic (par. 2.4)
- Adaptive Stability Map for wheel velocity selection (par. 2.5)

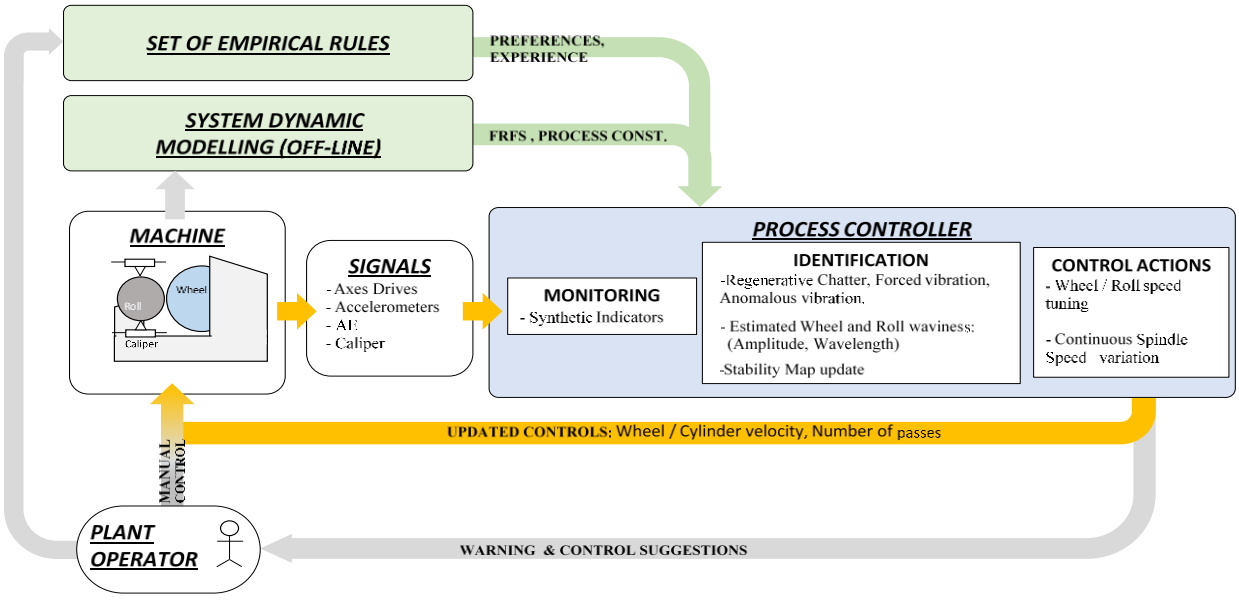

Figure 1. Machine controller architecture

2.1. Vibrations

Two types of regenerative chatter instability can appear in grinding, related to wheel and workpiece regeneration. In this study, roll grinding case is selected as a reference technological application. In this context, since in industry roughing operation and its multiple cutting passes along the cylinders are usually performed with high traverse speeds and reduced or null overlaps of

ground stripes, the possibility to incur in workpiece regenerative chatter is minimized: in fact, in this case any significant workpiece surface portion is subject to multiple passes, hence, for definition the surface cannot be regenerated. While during finishing operation chatter is usually controlled via conservative workpiece velocity, roughing must be performed with high workpiece velocity and infeed to increase productivity. Therefore, chatter appears mainly during the roughing phase and the proposed controller focuses only on *wheel regenerative chatter.*

Wheel regenerative chatter depends on wheel wear evolution. Engage a grinding wheel with radius R_s for removing a nominal constant infeed h_0 from the workpiece and let d_r be the corresponding wheel workpiece centers approach displacement (that considers both the commanded displacement and the elastic response of the structure under grinding force). Wheel wear varies along the wheel periphery and evolves during the time. As constant speed grinding is considered, wheel wear at the engagement point can be expressed as a function of time t only. The actual infeed $h(t)$ is then given by the following expression (Figure 2):

$$h(t) = d_r(t) - w(t-\tau) \tag{1}$$

where $w(t-\tau)$ is the radial wheel wear at the engagement point accumulated until time $t-\tau$. Wheel wear increment, going through the engagement region, can be expressed through the so-called Radial Grinding Ratio G_r. The Radial Grinding Ratio can be derived from the more common G-ratio G, representing the volumetric ratio between workpiece material removal rate Q_w and wheel total wear rate Q_s.

In fact:

$$G \overset{def}{=} \frac{Q_w}{Q_s} \Rightarrow G = \frac{\cancel{b} v_w h}{\cancel{b} v_s w} \Rightarrow \frac{w}{h} = \frac{1}{G}\frac{v_w}{v_s} \overset{def}{=} G_r \tag{2}$$

For a conventional aluminum oxide wheel in a roughing cutting operation on unalloyed steel, an average value of G-ratio is 10 as indicated by Marinescu et al. [27]; then, considering a typical ratio v_s/v_w=30 (Table 2), it yields G_r=0.003.

G_r states a proportionality between the occurred radial wheel wear and the infeed that has been engaged Eq.(3). Namely,

$$w(t) - w(t-\tau) = G_r \cdot h(t) \tag{3}$$

Moving to the Laplace domain, Eq.(3) becomes:

$$G_r \cdot h(s) = w(s) \cdot \left(1 - e^{-\tau s}\right) \Rightarrow w(s) = \frac{G_r \cdot h(s)}{\left(1 - e^{-\tau s}\right)} \Rightarrow w(s) \cdot e^{-\tau s} = \frac{G_r \cdot h(s) \cdot e^{-\tau s}}{\left(1 - e^{-\tau s}\right)} \tag{4}$$

Then, substituting $w(s) \cdot e^{-\tau s}$ into the Laplace transformation of Eq.(1), it yields:

$$h(s) = d_r(s) - \frac{G_r \cdot h(s) \cdot e^{-\tau s}}{\left(1 - e^{-\tau s}\right)} \Rightarrow \frac{h(s)}{d_r(s)} = \left(1 + \frac{G_r \cdot e^{-\tau s}}{1 - e^{-\tau s}}\right)^{-1} \tag{5}$$

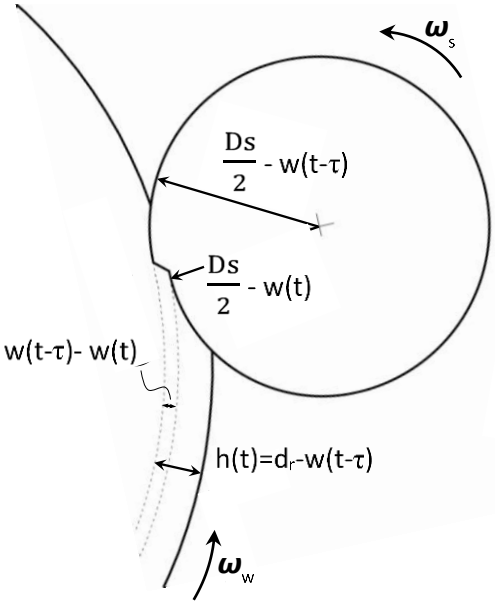

Figure 2. Grinding wheel wear mechanism

Eq.(5) provides the ratio between the required relative position and the actual infeed, usually reduced by the wheel wear. If system flexibility is considered, d_r will be varied by occurring relative vibrations between wheel and workpiece. Eq.(5) represents the ratio between the actual infeed (i.e., the depth of material stripe removed from workpiece) and the relative displacement between wheel and workpiece. When this ratio is equal to one, all the relative vibration amplitude between wheel and workpiece is translated into waviness on workpiece, while wheel geometry is preserved; when the ratio has null value, all the vibration amplitude is entirely translated into wheel lobes. An important characteristic of the Transfer Function (TF) expressed by Eq.(5) is its "localization" in frequency. In Figure 3, Eq.(5) is plotted in steady-state condition (namely, posing $s=i\omega$) with respect to the dimensionless parameter $\tau^* i\omega/(2\pi)$, for 2 different values of G_r.

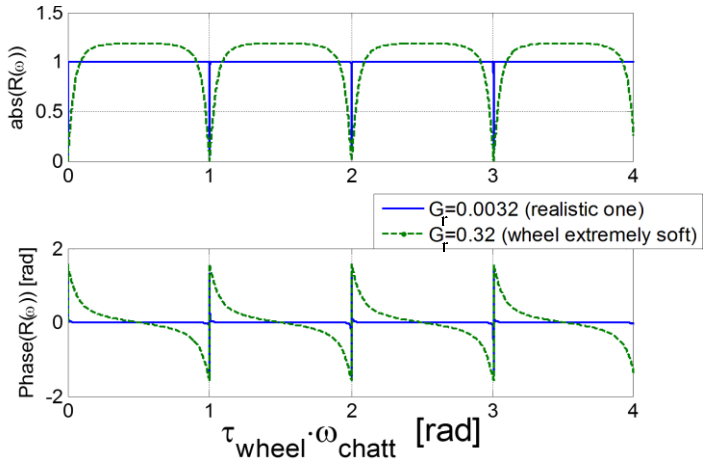

Figure 3. Comb filter of the grinding wheel regenerative chatter

It is clearly visible that wheel wear TF behaves as a comb-filter and it has effect on wheel waviness only if the vibration frequency is an integer multiple of wheel frequency ($1/\tau$). Therefore, wheel regenerative instability, that entails waviness growth on wheel surface, can happen only with chatter frequencies that are almost synchronous with a harmonic of the wheel frequency. The steepness of the comb-filter depends on G_r values: it is steeper as G_r becomes smaller. For typical values of G_r (e.g. the above-mentioned value G_r=0.003), the difference between chatter frequency and wheel harmonics is lower than 0.1%. The block diagram depicted in Figure 4 represents the wheel regenerative chatter dynamics. The model takes into account 2 DoFs: the displacements in normal and tangential directions, according to the approach proposed by Leonesio et al. [20]. These displacements are firstly perturbed by the vibrations induced by grinding force on the wheel-workpiece relative dynamics (i.e. $H(\omega)$) and wheel compliance (i.e. $1/k_c$); then, the sole displacement in normal direction (that it is assumed to coincide with the infeed direction) is modulated by wheel wear, whose occurrence decreases the actual infeed. Whereas grinding force is proportional to Material Removal Rate (*MRR)*, infeed modulation and infeed rate modulate force as well, that may increase the vibration level leading the system to instability.

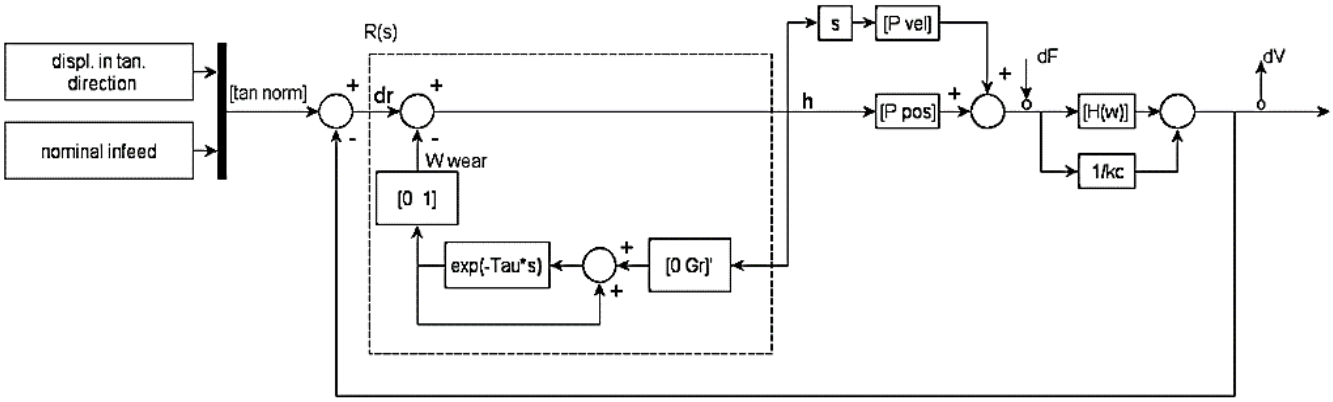

Figure 4. Block diagram of the grinding wheel regenerative chatter

The open loop system transfer function $L(s,\tau)$ is:

$$L(s,\tau) = R(s,\tau)\cdot\left(\left[P_{pos}\right] + s\left[P_{vel}\right]\right)\left[H(s)\right] \tag{6}$$

where $R(s,\tau)$ is the *TF* of the regeneration loop identified in Eq.(5) for a 1DoF system, that for a 2DoFs system assumes the following form:

$$h(s) = R(s,\tau)\cdot dr(s) = \left(I + \begin{Bmatrix} 0 \\ G_R \end{Bmatrix}\left(\frac{e^{-\tau S}}{1-e^{-\tau S}}\right)\begin{Bmatrix} 0 & 1 \end{Bmatrix}\right)^{-1}\cdot dr(s) \tag{7}$$

It can be observed that, in particular conditions, $L(s,\tau)$ can become unstable. According to the Nyquist criterion for Multi-Input Multi-Output (MIMO) systems, this is true when $det(L+I)$ makes clockwise circles around the origin. In other terms, if there exists a frequency ω such that $phase(det(L(\omega,\tau)+I))<180°$, the system is unstable. Consequently, the stability limit is traced by the solution of the Eq.(8):

$$\det(\mathbf{L}+\mathbf{I}) = 0 \tag{8}$$

Eq.(8) can be solved with respect to different combinations of process parameters, having kept the others constant, so that different stability charts can be obtained. In most of the cases, Eq.(8) can be solved only numerically.

Let the stability analysis be provided for the studied large traverse roll grinder. The Open-Loop relative dynamic compliance matrix between wheel and work cylinder has been measured, normal X and tangential Y directions has been considered as depicted in Figure 5.

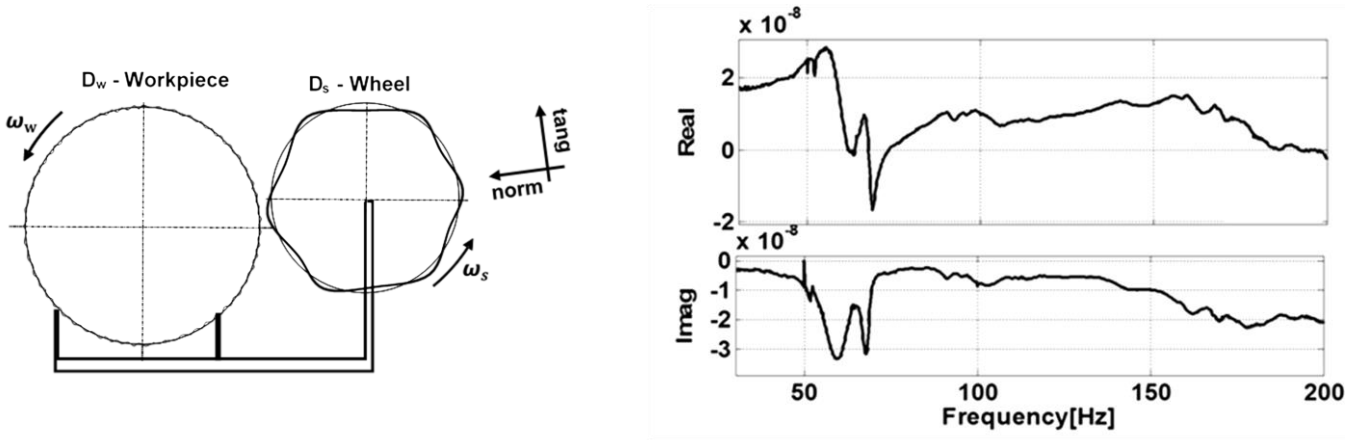

Figure 5. Machine structure scheme (LEFT) and measured FRF on the real machine in normal direction, H_{xx} (RIGHT).

The process matrices P_{vel} and P_{pos}, constituting the force model, assume the following expressions (Leonesio et al., 2014):

$$\mathbf{P}_{vel} = \frac{bk_t}{v_s}\begin{bmatrix} h & \sqrt{h\frac{D_w D_s}{D_w + D_s}} \\ \mu h & \mu\sqrt{h\frac{D_w D_s}{D_w + D_s}} \end{bmatrix} \tag{9}$$

$$\mathbf{P}_{pos} = \frac{bk_t}{v_s}\begin{bmatrix} 0 & v_w \\ 0 & \mu v_w \end{bmatrix} \tag{10}$$

Then, the parameter values outlined in Table 1 entirely define the cutting process (taken from the experimental tests presented in Section 3):

v_w [m/s]	v_s [m/s]	b [mm]	k_t [N/mm^2]	h_0 [mm]	μ	G_r	D_w [mm]	D_s [mm]
0.796	38	75	15000	0.003	2	0.003	700	430

Table 1. Grinding parameters considered for the stability analysis

The Nyquist plot of the given process is depicted in Figure 6. It can be noted that the diagram encircles the origin, thus, the closed loop process will be unstable. In particular, the part of the diagram bunging on the left, ultimate responsible of the encirclement, is ascribable to the regeneration TF of Eq.(7). As highlighted in the plot, this circle is mapped by a very small frequency interval (tenths of hertz), and the corresponding frequencies are quasi-harmonics of the wheel frequency (for instance, 69.31 /17.2797 = 4.00064).

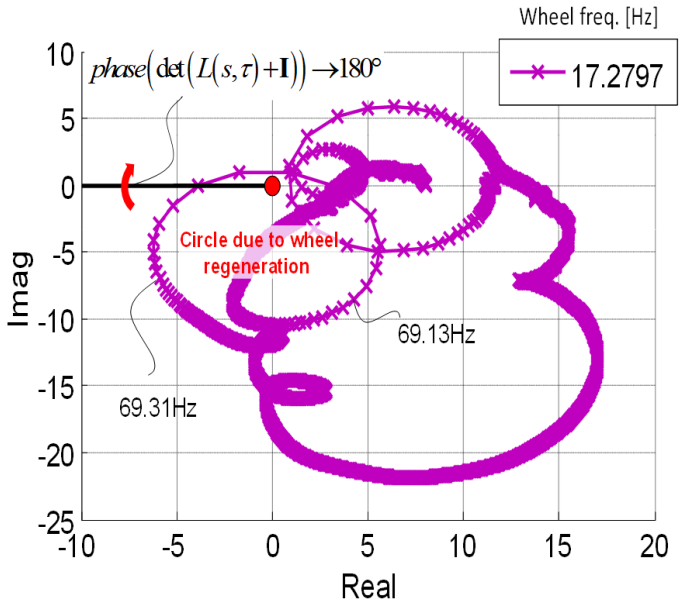

Figure 6. Nyquist stability diagram of the system machine + process: det($\mathbf{L}(s,\tau)$+$\mathbf{I}$).

Solving Eq.(8) w.r.t. width of cut (*b*) and wheel rotational speed, the stability chart of Figure 7 is obtained. Since the Eq.(8) is complex and transcendental, there exist infinite periodic solutions, one for each integer ratio between chatter frequency and wheel speed, corresponding to the formation of an integer number of lobes around the wheel. The points above the curves correspond to unstable grinding passes, while the points below correspond to stable ones. Each resonance generates a "train" of curves (lobes), one for each harmonic; between the lobes there are some stability pockets, i.e. "privileged" wheel velocities that allow a stable grinding for higher width of cut. The controller to suppress chatter onset exploits this latter property.

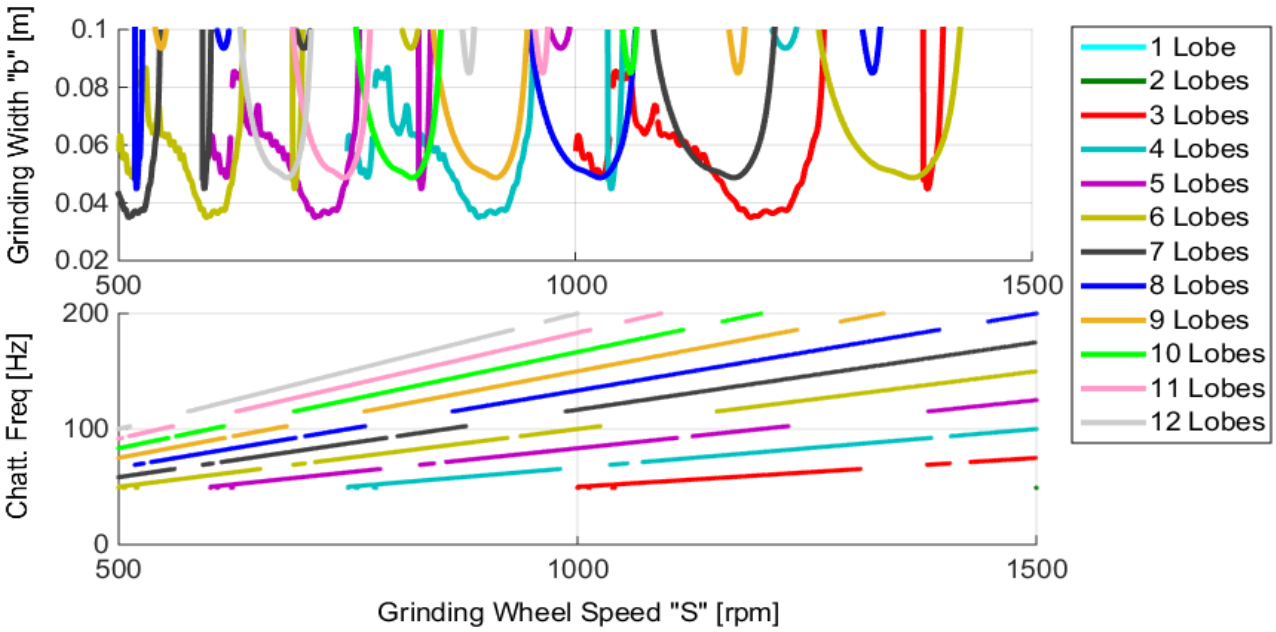

Figure 7. Computed Stability Chart for the grinding process

2.2. Chatter Indicators

Based on the considerations expressed in the previous paragraph, a Fourier-domain indicator based on synchronous content for chatter detection in traverse grinding (*ChatInd*) has been designed, able to point out vibrations induced by wheel regenerative chatter. Similar approaches, based on the synchronism properties in frequency domain of the stable/unstable machining vibration, have already been applied in other machining processes such as turning and milling, to rapidly identify the onset of regenerative chatter (Van Dijk et al., [28]). The big difference in the monitoring algorithm relies on the fact that in turning and milling, the regenerative chatter induces vibrations that are generally not synchronized with the rotational speed of the spindle and with its multiple harmonics and therefore chatter can be identified when asynchronous vibration rise up during machining. On the opposite side, as demonstrated above for grinding, this quasi-synchronism appears when wheel regenerative chatter triggers and therefore the synchronous vibrational energy becomes a good indication for chatter diagnostic.

Mathematically, the developed chatter indicator is defined as follows:

$$\mathrm{ChatInd}_k = \frac{\sum_{N_j=N_{\min}}^{N_j=N_{\max}} \sum_{\omega_i=N_j\cdot\omega_s-\Delta\omega}^{\omega_i=N_j\cdot\omega_s+\Delta\omega} \frac{\left|\ddot{X}_k(\omega_i)\right|}{\omega_i^2}}{\sum_{\omega_i=\omega_{\min}}^{\omega_{\max}} \frac{\left|\ddot{X}_k(\omega_i)\right|}{\omega_i^2}} \tag{11}$$

where:

- N_{max}, and N_{min} are respectively the maximum and the minimum number of wheel harmonics to be considered in the signals $\ddot{X}_k(\omega_i)$;
- $\boldsymbol{\omega}_s$ is the actual wheel angular velocity in rad/s;
- $\Delta\omega$ is the half-width of the considered frequency interval, around a wheel harmonics, used as selection windows for the synchronous component of each band.

When signal $\ddot{X}_k$ are produced by accelerometers, the chatter indicator is based on the relative displacement obtained by a double integration and an appropriate structural transmissivity function because displacement amplitude is directly linked to the formation of surface waviness, thus representing a more significant quantity.

This indicator, thanks to its simplicity and computational lightness, enables a soft real-time process monitoring that is integrated in the process controller for triggering the activation of the unstable cutting state.

Several *ChatInds* are computed for different acceleration signals and they are composed via proper weights to be calibrated during controller initial tuning Eq.(12).

$$\mathrm{ChatInd} = \sum_k w_k \cdot \mathrm{ChatInd}_k \tag{12}$$

The idea is that the w_k weights coefficient (i.e. positive real numbers $0 < w_k < 1$) could be used to maximize the overall sensitivity to detect process vibration when different type of accelerometers (with different sensitivities and bandwidth, in relation to the modes shapes involved in the vibration) are used. In the tested machines k=1,2,3 and $w_1=w_2=w_3=1/3$, since three similar accelerometers were adopted. While *ChatInd* is suited to track the level of developed chatter vibrations, in principle at the beginning regenerative instability occurs with a zero energy level, so that the conceived indicator may lack promptness. However, it can be demonstrated that wheel regenerative chatter is characterized by a low growth rate. Assuming that a wheel-workpiece relative sinusoidal vibration is imposed, Eq.(5) describes the effect of wheel wear evolution on the ratio between the

required sinusoidal infeed and the actual one. Exploiting a 1st order Padè approximation, the time constant of the dynamical system describing wheel wear evolution is given by Eq.(13):

$$T_p = \tau \frac{1 - G_R}{G_R} \tag{13}$$

The chatter time constant T_p represents the time in which the system reaches the 60% of its steady-state value: for instance, considering the previous radial grinding ratio G_r = 0.003, Eq.(13) estimates that the actual infeed reaches around the 60% of the final value due to wheel wear in about 300τ seconds i.e. 300 wheel revolutions. Therefore, the derivative is small compared with the instantaneous amplitude.

Preliminary experiments on the test grinder (par. 3.1) confirm good diagnostic capacity of the proposed chatter indicator. Eight different values of wheel speed were adopted on the test machine for a semi-roughing grinding cycle (with cylinder velocity V_w=28 rpm, nominal infeed h=8 μm, no wheel overlap). Each wheel speed value has been maintained for at least 10 grinding passes in order to allow accumulation of the waviness for unstable speed values. After the passes, the cylinder has been measured by means of the machine caliper to verify whether waviness was accumulated on the roll, to confirm chatter onset. In three of the eight tested speeds, wheel regenerative chatter occurred (red marks in upper diagram of Figure 8). In fact, in all these three chattered cycles, the chatter frequencies were multiple of wheel harmonics in agreement with the exposed wheel regenerative chatter theory (par. 2.1). Chatter Indicators during those three tests showed a sharp increase above 50% and a threshold could then be defined in the controller for the identification of the chatter onset. A threshold value ranging from 50% to 75% resulted appropriate for a wide range of situations (different wheel and workpiece types and dimensions, different cutting parameters).

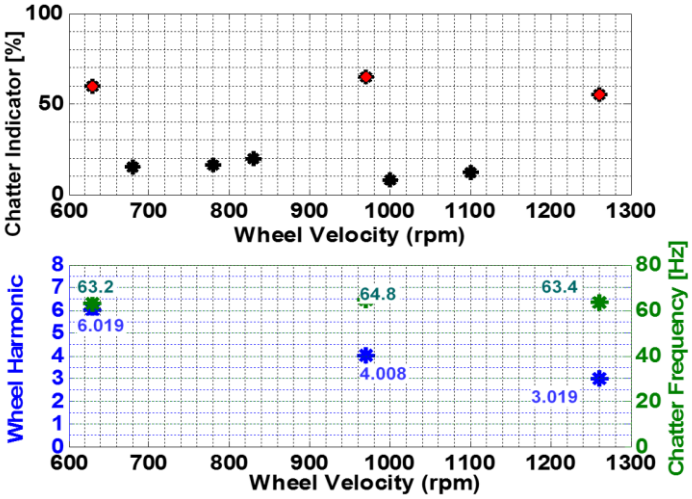

Figure 8. Chatter Indicator values for different wheel velocities (experimental tests)

2.3. Waviness observer

A useful capability of the process controller is producing an indirect quantification of the resulting waviness on the roll and wheel during the process, avoiding the interruption of the cutting operation to measure the workpiece by the standard caliper. The estimation of the surface waviness is directly used by the described process controller, but also constitutes a significant real-time surface quality indication for machine operators. The so-called "waviness observer module" (*WavObs*), presented by Parenti et al. [29] has been integrated in the process controller as a brick of the process monitoring layer. This algorithm estimates workpiece and wheel waviness in traverse grinding by adopting a dynamic model-based approach to process the acceleration signals captured on the machine. This module is integrated in the control logic but it must be stressed, nevertheless, that the proposed process adaptive controller can be implemented independently of the *WavObs*, adopting approximated waviness indicators based on the raw acceleration signals, without taking into account the structure transmissibility.

The *WavObs* algorithm exploits a linear model of machine and process dynamics and a Least Squares identification method in the frequency domain. As stated, waviness causes a relative oscillation between wheel and workpiece. A series of accelerometers installed on the grinder can quantify those displacements by applying a double integration in time-domain. To achieve the estimation of the wheel/workpiece contact point relative displacement, each accelerometer reading must be transformed considering the corresponding transmissibility function (since the sensors are installed in different machine positions, they are linked to the contact displacement by different responses due to the machine dynamic behavior). Once the relative "process" displacement is obtained, knowing the closed-loop response of the machine and grinding process (Figure 4) the actual waviness on the wheel and cylinder is estimated.

The waviness on the wheel and the roll side, and in particular the complex coefficients $a_{S,}\, a_W$ that describe both their amplitude and their phase, are estimated by the observer by inverting Eq.(14). This equation mathematically describes the measured acceleration $\ddot{X}_{sens}$, in the Fourier domain:

$$\ddot{X}_{sens}(\omega)=T(\omega)\cdot i\omega^2\cdot \mathrm{H}_{\mathrm{NCL}}(\omega)\cdot\left\{\Im(\Delta h_{Sj}(\theta_S)) \quad \Im(\Delta h_{Wj}(\theta_W))\right\}^T\cdot\left\{a_{S_j} \quad a_{W_j}\right\} \tag{14}$$

Where:

- $\mathrm{H}_{\mathrm{NCL}}$ is the radial closed-loop structural response, obtained by joining the measured machine response (Figure 5) with the grinding process model in Eq.(9) and Eq.(10).
- T is the measured transmissibility function of the sensors.

- $\Delta h(\theta)$ is the radial displacement in the contact zone of the wheel and the workpiece
- $\Im$ indicates the Fourier transform with the complex variable ω.

Experiments proved that this method guarantees good results on the tested roll grinding machine (Parenti et al. [29]) and that a good on-line estimation of the waviness can be achieved. The following paragraph describes the control logic and how the estimated waviness is exploited.

2.4. Control logic

The control logic is described by browsing each state of the control state machine and describing the associated actions and transitions. States are organized in logical regions, each one pertaining to a particular system condition. Regions are described in the order they are accessed during a typical work-cycle exhibiting chatter problems.

Region 1: "Vibration monitoring"

Region 1, named "*Vibration monitoring*", is devoted to establish whether a vibration problem is occurring. When the system experiences low vibrations level, no control action is required. Anomalous vibrations are recognized by computing acceleration RMS, and the "High Vibration" state is activated (Figure 9): this does not mean that regenerative chatter is occurring, since vibration onset may be associated to other causes, like external disturbances, surrounding vibration, component defects (for instance, workpiece driving system irregularities), etc.

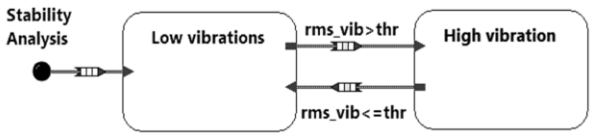

Figure 9. State machine – region 1: "Vibration monitoring"

Regions 2, "Control Logic", and 3: "Waviness Analysis"

Regions 2 and 3, named "*Control Logic*" and "*Waviness Analysis*" respectively, represent the kernel of the control logic: they must discriminate if the occurring vibrations are due to wheel regenerative chatter, in order to exert - if required - specific control actions. They are accessed in parallel when the "*High-vibration*" state is active, in region 1. Starting from nominal velocities for wheel and workpiece, if *ChatInd* exceeds a given threshold (transition B1→B2), two parallel actions are carried out: Spindle Speed Selection "*SST Selection*" and Waviness Observer Calculation "*WavObs Calculation*" (Figure 10).

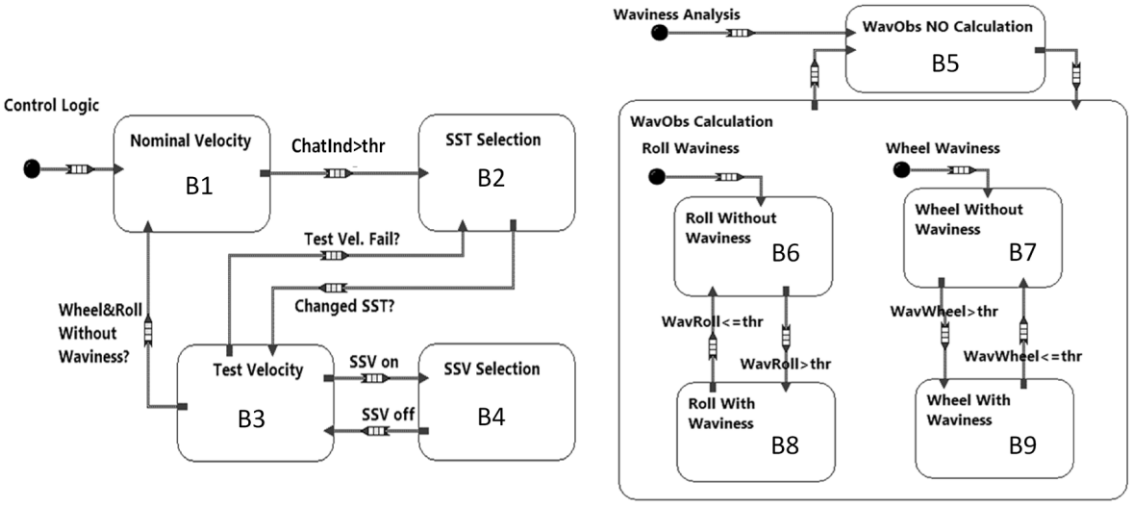

Figure 10. State machine – Regions 2, “Control Logic”, and 3: “Waviness Analysis”

“*SST Selection*” state (B2) selects a new wheel velocity aiming at stabilizing the system. The selection is performed querying an adaptive stability map (*SM*) which contains a score for each possible wheel velocity (discretized in bins) in a feasible technological window: the velocity with the best (highest) score is chosen for stabilizing the process. At the same time, the *SM* is updated penalizing the wheel velocity that provoked chatter occurrence. The criteria for the assignment of the scores and the *SM* adaption/evolution strategy are presented in the next paragraph.

While chatter mitigation strategy, either *SST* (Spindle speed tuning) or *SSV* (Spindle speed variation), is applied, the generated waviness is monitored by means of the "*Waviness Observer Calculation*" (B5→ B6 B7 B8 B9). To discriminate between waviness on wheel and roll sides, a shift in speed is required to assure waviness observability on the two sides. The "SST Selection" itself activates a wheel speed shift to suppress chatter, making the two waviness observable. In parallel, the *Waviness Observer* module identifies, logs and processes the chatter frequency permitting the evaluation of the residual amplitudes. When these actions are performed, the system goes into the "*Test Velocity*" state (B2→B3). In this state, the controller keeps calculating the *ChatInd* (that monitors the possible onset of new waviness with different wavelength related to the new wheel velocity) and the amount of existing waviness, respectively. No changes in the cutting parameters are generated in B3 state, while its exit conditions are based on the following quantities:

- Low waviness amplitude on the Roll and Wheel (i.e. meaning that waviness has been canceled out)
- *ChatInd* grows over the threshold (i.e. when a new chatter frequency rises in the signals spectrum)
- "*SST iterations*" reach the limit number: “*SST iterations*” is a "counter" associated to the number of "*SST attempts*" (i.e. the number of unsuccessful speed tuning attempts).

The first condition verifies whether the existing waviness has been canceled within a reasonable time (the threshold is decided by the operator but could also be optimized automatically). If the number of grinding passes, defined in the work cycle, terminates before the above-mentioned chatter suppression period, the controller adds new passes until reaching the prescribed time or until the vibration goes under a prescribed level. According to *WavObs* estimation, an automatic dressing cycle is launched when the waviness accumulated on the wheel surface is too high: this is usually not the case, because a stable cutting speed eliminates the waviness also on the wheel side. The second condition makes the system able to deal with new chatter frequencies that can rise up in the spectrum unexpectedly with the selection of the new cutting velocity. When the first and second conditions are both activated, namely the waviness is low and no new chatter frequency appears in the spectrum, the controller moves back to the "*Stable Cutting*" state; otherwise moves to "*SST Selection*" (B3→B2) that re-applies a new speed shift. If this latter loop is executed a predefined number of times (typically 3) and no stable velocity is found, the system switches to the "*SSV Selection*" state (B3→B4), that launches another chatter mitigation technique based on *Continuous Spindle Speed Variation* (Alvarez et al., 2011). Frequent occurrences of this latter action suggest possible accuracy problems with the machine dynamic model that is adopted from the controller for producing the waviness estimation. Therefore, at the end of the cycle, a verification of the machine dynamic through frequency response measurement is prescribed to the operator. In case the system experiences a transition to "*Unstable Cutting*" during the cycle, a direct measurement of the cylinder by means of the machine caliper is also prescribed at the end of the cycle, for quality acceptance purposes.

2.5. Stability Map

The Stability Map (*SM*) is the knowledge base exploited by the controller to select a stable wheel velocity. It can be represented by a plot bar having wheel velocity as discretized abscissa and a dimensionless merit factor (score) in the ordinate (Figure 11), where -1 corresponds to high instability and +1 to a stable cutting speed. The *SM* has been designed to exploit synergistically a priori and in-process information.

The *SM* can be initialized based on a stability chart computed starting from dynamic compliance measurements, e.g. by impact testing, and estimated process parameters, as shown in Figure 7. Of course, process parameters have to be measured for each wheel-workpiece configuration and type. Alternatively, the *SM* can be simply initialized to a homogeneous value of zero, leveraging on the controller fast convergence toward an effective *SM* by continuous map updating (Figure 11).

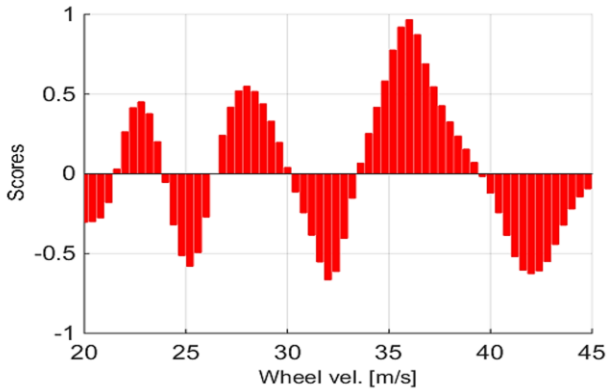

Figure 11. Experimental Stability Map of the test machine

SM Updating

The stability map is updated whenever the "*Test Velocity*" state, presented in the previous paragraph, accomplished its task classifying the current wheel velocity as stable or unstable. Figure 11 is obtained experimentally on the tested machine (par. 3.1), by starting from a flat map initialization. The same cutting configuration adopted for chatter indicator tests of Figure 8 has been considered, except the nominal infeed values which has been varied from a =3 μm to a =20 μm. In addition, manual periodic wheel dressing has been carried out to reproduce typical industrial use. In the executed tests, the update process of Figure 11 was induced by manually selecting a wide range of initial wheel speeds (ranging from V_s=20 m/s to V_s=45 m/s), similarly to what has been done in the final experimental campaign (Tables 2-3-4).

Each time the "*SST selection*" state is left, the *SM* scores are updated through a weighted average with the previous scores stored in the map:

$$OSM_t(\mathbf{v}) = \alpha \cdot OSM_{t-1}(\mathbf{v}) + (\alpha - 1) \cdot US_t(\mathbf{v}) \tag{15}$$

where:

- OSM_t is the original stability map assigning a score to each element of the vector of the possible wheel velocities **v** (by a proper discretization of the technologically feasible range)
- $US(\mathbf{v})$ is the vector of the updated scores derived from process monitoring
- α is a weighting factor ranging from 0 to 1 that aims at balancing the importance of the new scores with respect to previous ones; subscript t scans the update events as determined by the *SM* controller. The α coefficient has been fixed to 0.9 in the experiments.

As already discussed in the previous paragraphs, if the chatter indicator overcomes a given threshold (typically 50%), a chatter frequency is identified and the current wheel velocity is labeled as unstable and a negative score is assigned to it (e.g. -1). Softer

negative scores (i.e. -1<U(v)<0, typically 0.7) are assigned also to all wheel velocities whose revolution frequency is a submultiple of the chatter frequency, since they are also critical according to chatter theory, because they generate wheel waviness with an integer number of periods in one revolution. On the other side, if the chatter indicator does not raise after a predefined amount of time the wheel velocity is confirmed as "stable" and a positive score is assigned to it; since the chatter frequency is undefined, in this case the positive score is assigned to the sole tested velocity.

Data aging

Assuming that reliability of *SM* scores assigned at time $\bar{t}$ decreases as time goes by, because the probability of process or machine variation increases, the *SM* is subject to a forgetting law. Every "epoch", whose extension may be quantified in days, weeks, or months, the overall *SM* is attenuated by a γ<1. Mathematically:

$$OSM_e(\mathbf{v}) = \gamma \cdot OSM_{e-1}(\mathbf{v}) \tag{16}$$

where subscript *e* scans the epochs. Let Δe be the time span between epochs and the quantity $\gamma \cdot \Delta e$ the time constant of the exponential attenuation provided by the forgetting law. A proper choice of the time constant is not a trivial task: a long "beta testing" period is necessary to frame the evolution rate of the machine system. Moreover, whereas a pure time aging could be meaningless if the machine is kept unused, an event-based aging approach can be adopted: in this case, the subscript *e* scans some significant events in grinder "life", e.g. maintenance activities and/or machine spare parts replacements. Hybrid solutions are also possible.

SM smoothing for robustness

In principle, *SM* updating may produce a very scattered map: indeed, very positive wheel velocities could lie near very negative velocities. In this case, a slight misplacing of the scores due to unavoidable fluctuations may mislead the control action. Then, in order to increase the robustness of the control action, the best wheel velocity, that is the velocity with the highest score, is sought in a "smoothed" stability map (denoted with *SSM*) obtained from the original one applying a moving average filter (order 2), each time the map is updated. In this way, stable velocities surrounded by unstable velocities will be penalized and avoided.

SM and operator choice

In grinding practice, the wheel velocity is usually chosen for fulfilling technological requirements that are not related to chatter, but with other process performance like surface roughness, burnings, productivity, etc. Thus, it is straightforward that if two velocities in the *SM* have similar scores, the one nearer to the nominal velocity decided by the operator should be preferred. The

operators usually defines a technological window taking into account the characteristics of the adopted grinding wheel and her/his experience.

This logic is implemented by correcting the Smoothed Stability Map with a supplementary score addendum provided by the machinist. Then, the resulting final *SM* (denoted with *FSM*) is given by the following expression:

$$FSM_t(\mathbf{v}) = \beta \cdot SSM_t(\mathbf{v}) + (\beta - 1) \cdot OS_t(\mathbf{v}) \tag{17}$$

where β is a weighting factor ranging from 0 to 1 that aims at balancing the importance of the scores related to chatter and the scores expressing operator preferences; OS_t(v) contains the scores that the operator assigns to the wheel velocity at time *t*. Since operators usually indicate only one nominal velocity, the *OS* vector can be computed as a "bell" function (i.e., a Gaussian distribution) centered on this nominal value.

3. DEMONSTRATION ON AN INDUSTRIAL ROLL GRINDER

3.1. Machine and cutting cycle setup

Experimental tests were executed on an industrial medium size roll grinder setup with the standard configuration (i.e. coolant, dressing parameters, machine setup etc.) for machining hot mill steel rolls. An aluminum oxide wheel (458AG07H6B1) of diameter D_S=660 mm and width b=70 mm and a High Chromium Cast Steel (HSS with grade KV5) with 45 HRC of hardness and D_w=492 mm of diameter with straight profile (total length L_T=2400 mm), were adopted. The machine dynamic was first characterized by using impact-testing technique and preliminary cutting passes have been carried out to calibrate the waviness observer module. The machine was equipped with three triaxial acceleration sensors (PCB 356B18 with sensitivity of 1 V/g) installed on the two machine neckrests (that support the roll during rotation) and on the wheel head carriage.

3.2. Implementation of the controller

The process controller has been implemented on a real-time National Instrument™ Platform (Compact DAQ) by exploiting the LabView™ Software (Development Kit, Real-time and StateChart programming modules). Connection with the accelerometers installed on the machine is done by 3 acquisition boards (NI 9234 IEPE, 4 channels each, with anti-aliasing filtering and simultaneous sampling) acquiring signals at 4 KHz.

Connection with the machine supervisor and machine numerical control adopts a TCP/IP protocol to read/write the cutting cycle parameters and to access all the actual displacement/speeds/currents of the machine axes (with 500 Hz bandwidth).

3.3. Preliminary Tests

Two different test cases have been preliminary considered for testing the process controller: the first (case #1) is a typical roughing cycle with aggressive parameters, whilst the second (case #2) is a semi-finishing grinding.

In case #1, chatter vibration rises up quickly in the spectrum at 61.8 Hz and the Chatter Indicator promptly detects it. Vibration accumulates into the system and chatter indicator increases, reaching the threshold (50%) for roughing cycles, after 5 grinding passes. The control system then switches to "*Unstable Cutting"* and therefore a shift in wheel speed is applied, moving from 930 rpm to 1064 rpm, prescribing also a Caliper measurement at the end of the cycle. At the same time, the *waviness observer* estimates around 6 µm of waviness, on both the wheel and the roll side (that reduces over time, after the new wheel speed has been adopted), reaching the minimum threshold, fixed at 0.5 µm, after almost 150 s. After that, the grinding parameters are kept constants, since the Chatter Indicator, now tuned on 1064 rpm (17.7 Hz), keeps below the threshold. At the end of the cycle, the caliper measurement detects no waviness on the roll surface, confirming the improved final quality achieved.

In case #2, less demanding cutting parameters are initially adopted, leading to less severe chatter conditions. After three passes chatter occurs at the same frequency (61.8 Hz), since wheel velocity is unvaried between cycles, with 0.7 µm of estimated amplitude in relative oscillation between wheel and roll. For semi-finishing or finishing operations, the threshold on the *chatter indicator* (to trigger the automatic speed tuning) along with the threshold for the waviness are fixed at 0.2 µm.

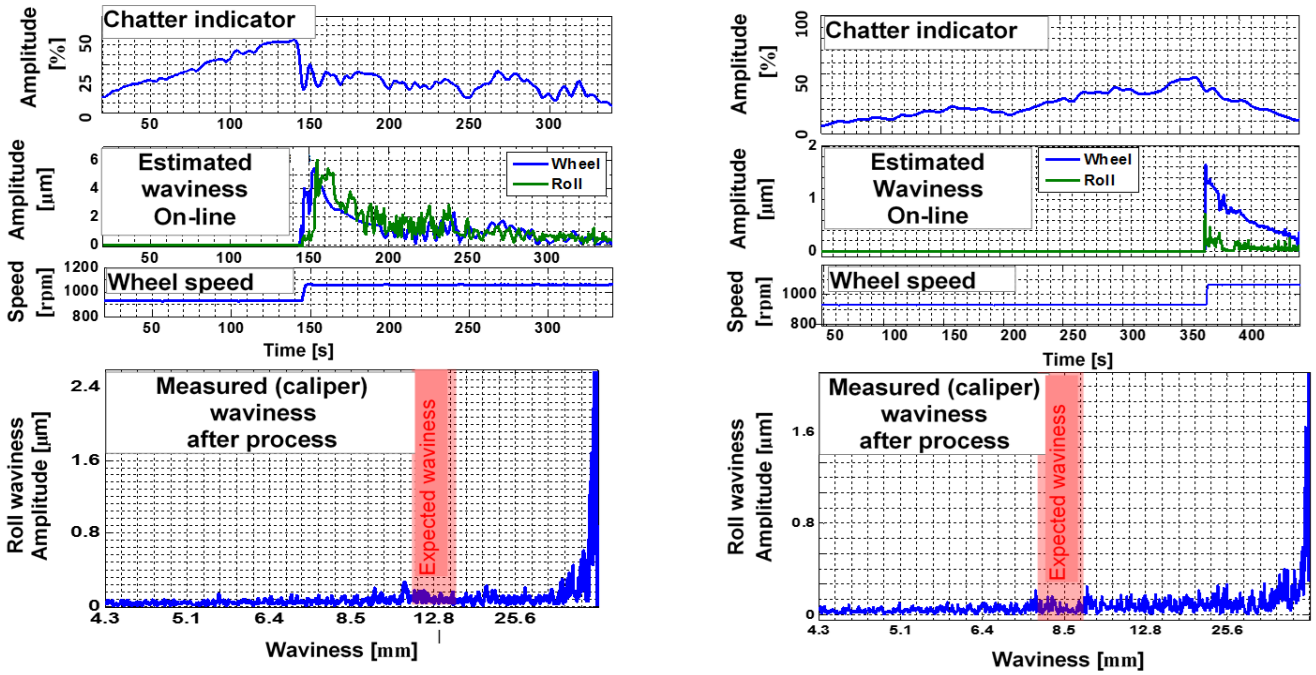

Figure 12: Chatter indicator during experimental test case #1 and case #2 on the roll grinder, Caliper measurement for waviness detection, performed at the end of test case n°1 and n°2

The same good performance of the controller is showed in cycle 2, meaning that even in presence of passes overlap the vibration can be suppressed assuming wheel regenerative chatter as the underlying phenomenon. The detected roll waviness is smaller than in cycle 1, as well as the decreasing rate of the waviness when speed tuning is applied. At the end of the cycle, according to the estimation of the *waviness observer* and to the caliper measurement, the workpiece is free of waviness defects (Figure 12).

3.4. Experimental Campaign

Based on the good results achieved on the preliminary cutting tests, an extensive experimental campaign has been carried out to test the controller performance and the automatic chatter control.

Grinding cycles typically adopted in roll grinding for hot mills are made of several different phases, starting from roughing, passing through semi-finishing and leading to finishing and spark-out operations. In order to cover all possible technological situations, validation experiments are composed by three different test types, described in Table 2 as Type A, Type B, and Type C. Type A is roughing, where high Material Removal Rate is needed for maximizing productivity. Type B is semi-finishing, where the cutting pressure is reduced in order to improve surface quality. Finally, Type C is finishing, where high wheel overlap is used to get the required accuracy and surface quality.

The 14 executed tests are characterized by different starting wheel speeds that are known to generate a stable or unstable cutting basing on the adaptive stability map and on empirical knowledge gained during previous experiments. Small perturbations are also introduced on the initial values in order to test a wider technological area and to provide fictitious uncertainty in the choice to test the process control robustness. These perturbations were introduced either on the wheel speed, on the cylinder speed, and on the nominal end infeed values, randomly extracted from continuous Gaussian distributions with standard deviation σ=1 m/s for the wheel speed, σ=1 rpm for the cylinder speed and σ=1 μm for the nominal end infeed. However, in the latter two cases, the perturbations have been limited to integer values, given the resolution of the machine numerical controller: 1 μm and 1 rpm, for the infeed and the cylinder speed, respectively.

	***Type* A**	***Type* B**	***Type* C**
Wheel speed	Medium-High (30-40 m/s)	Medium-High (30-40 m/s)	Medium-Low (22-27 m/s)
Cylinder rot. speed	Medium-Low (22-24 rpm)	Medium-Low (22-24 rpm)	Medium (30 rpm)
Nominal Infeed	Medium-High (~0,015 mm)	Medium-Low (~0,006 mm)	Low (~0,003 μm)
Relative workpiece overlap	Null (0%)	Low (10%)	Medium (40%)
Programmed Cutting passes	20	4	1

Table 2: Cutting cycle types definition for validation tests of the process controller

For each test the roll waviness has been directly measured before and after the machining test by the machine caliper (in a similar way as done for the waviness observer module validation) in order to get the initial and final surface qualification.

Two different types of surface indicators are extracted from spiral caliper measurements along all the cylinder length. Each profile has been decomposed into form, waviness, and roughness profiles by means of a Gaussian filter (GPS ISO 12181, [30]), in order to analyze the roundness profile deviations. However, only waviness and geometric effects are actually taken into account in the analysis (separated by a cut-off wavelength of 32 mm), due to the limits of the contact caliper that is not suitable for measuring very small wavelengths belonging to roughness range (cut-off wavelengths at 0.8 mm). In the studied industrial scenario, a threshold for the waviness amplitude can be defined at 1 μm: below this value cylinders are considered as good from grinding operators and quality controllers. Table 4 presents the results, where last column indicates the intervention of the controller for stabilizing the process. In six different tests, chatter was correctly identified and wheel speed was adjusted stabilizing the process. In test ID6, after two different automatic speed tuning control actions, the roll was free of defects at the end of the cycle indicating the good effectiveness of the strategy. The corresponding evolution of the chatter indicator and the selected wheel speed are reported in Figure 13.

In all tests visual inspections and surface finishing judgments by experienced operators have been also conducted, confirming that no waviness were formed thanks to the appropriate control actions carried out by the controller, as depicted also by the following Figure 14. The same good performance is achieved in terms of geometrical accuracy, as shown by the "Geometry" indices in Table 4.

Together with the results in terms of process performance, it is interesting to analyze the self-learning capabilities of process controller by tracing the evolution of the stability map across various stable and unstable tests. A synthesis of *SM* state evolution obtained during a preliminary training session (with tests of type A, roughing) is given in Figure 15: velocities have been selected by the operator, monitoring then the controller reaction.

Test ID (Run order)	Cycle type	Lobes number at principal chatter freq. (Hz)	Wheel velocity [m/s]	Wheel velocity perturbed [m/s]	Roll velocity [rpm]	Roll velocity perturbed [rpm]	Relative workpiece overlap[%]	Traverse velocity [mm/min]	End infeed [mm]	End infeed perturbed [mm]	Number of programmed passes
1	C	~4,5	27,7	27,8	30	30	40	1417	0,003	0,003	1
2	C	~5,5	22,7	22,1	30	29	40	1326	0,003	0,003	1
3	A	~3	41,6	41,5	22	21	0	1753	0,015	0,014	20
4	B	~3	41,6	41,6	24	23	10	1715	0,005	0,005	4
5	C	~5	25,0	25,2	30	31	40	1372	0,003	0,003	1
6	A	~3	41,6	41,1	22	22	0	1676	0,015	0,013	20

7	B	~4,5	27,7	27,7	24	23	10	1646	0,005	0,005	4
8	A	~3	41,6	40,8	22	22	0	1753	0,015	0,017	20
9	A	~4	31,2	31,3	22	23	0	1753	0,015	0,013	20
10	A	~4,5	27,7	27,7	22	21	0	1676	0,015	0,013	20
11	A	~3,5	35,7	35,2	22	21	0	1753	0,015	0,013	20
12	B	~3,5	35,7	35,2	24	24	10	1577	0,005	0,005	4
13	C	~4	31,2	31,6	30	29	40	1417	0,003	0,003	1
14	B	~4	31,2	31,5	24	23	10	1577	0,005	0,005	4

Table 3: Detailed tests parameters for validation of the process controller

Stable velocities, whose neighbor bins are thus filled with positive scores, characterize tests 1 to 3. From now on, the controller will propose to select these velocities to stabilize the process. If the operator imposes an unstable velocity (test ID4), after the foreseen control cycle this velocity is labeled as unstable: a negative score is assigned to it and to all the related harmonics and/or sub-harmonics (in attenuated form); then, the controller switch to a stable velocity (test ID5). Wherever the operator selects another unstable velocity, this velocity is further penalized (test ID8). The final *SM*, obtained after 25 tests, has been already presented (par. 2.5, Figure 11). The performance of the controller is confirmed by visual inspections after the tests (e.g. test ID6, Figure 14). The presented *SM* evolution shows how, in few attempts, the controller is able to reconstruct a complete stability chart with all the relevant stability pockets predicted by chatter theory. Therefore, as stated in par. 2.5, the initialization of *SM* with the diagrams coming from the analytical approach outlined in par. 2.2 is not mandatory and does not affect the overall controller performance.

Test number	Cycle type	Waviness (µm)		Geometry (µm)		Chatter freq. (Hz)	Number of controller interventions on the wheel velocity
		RMS	**MAX**	**RMS**	**MAX**		
3	A	0,25	1,11	1,00	7,07	60,2	1
6	A	0,31	1,02	0,57	3,53	60,8/66,5	2
8	A	0,23	0,84	0,47	3,45	62,5	1
9	A	0,21	0,97	0,48	3,63	60,3	1
10	A	0,31	1,14	0,84	4,23	-	0
11	A	0,23	1,05	0,58	3,36	68,9	1
4	B	0,16	0,52	0,44	3,51	-	0
7	B	0,20	0,68	0,47	4,47	-	0
12	B	0,21	0,67	0,50	3,68	-	0
14	B	0,19	0,79	0,48	3,51	-	0
1	C	0,16	0,56	0,45	3,44	-	0
2	C	0,13	0,57	0,46	4,17	-	0
5	C	0,17	0,65	0,46	3,87	-	0
13	C	0,12	0,41	0,37	3,42	-	0

Table 4: Results of the experiments of Table 3 in terms of geometrical features measured by machine caliper after machining

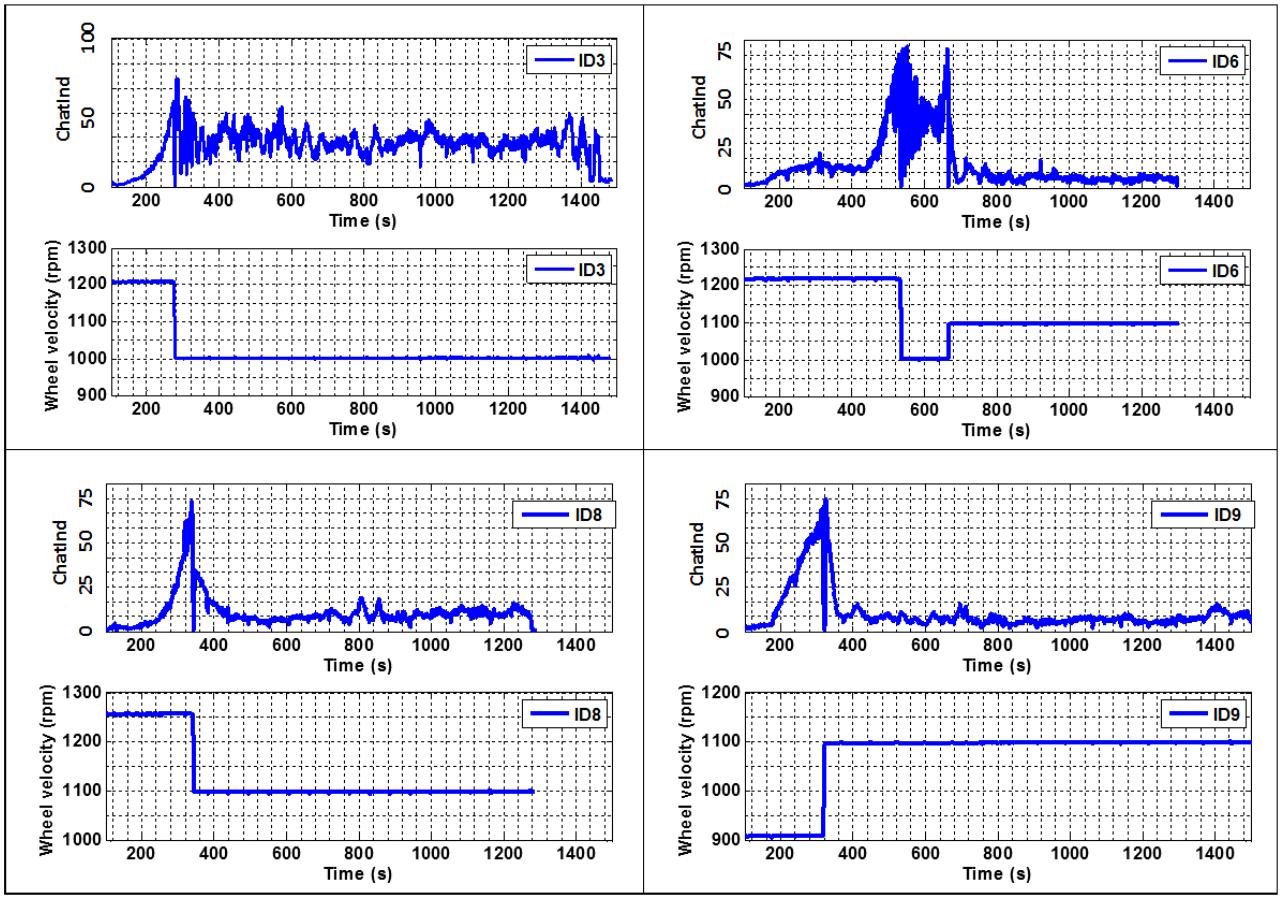

Figure 13: Chattered grinding test suppressed by the process controller. Test Number:ID3, ID6, ID8,ID9.

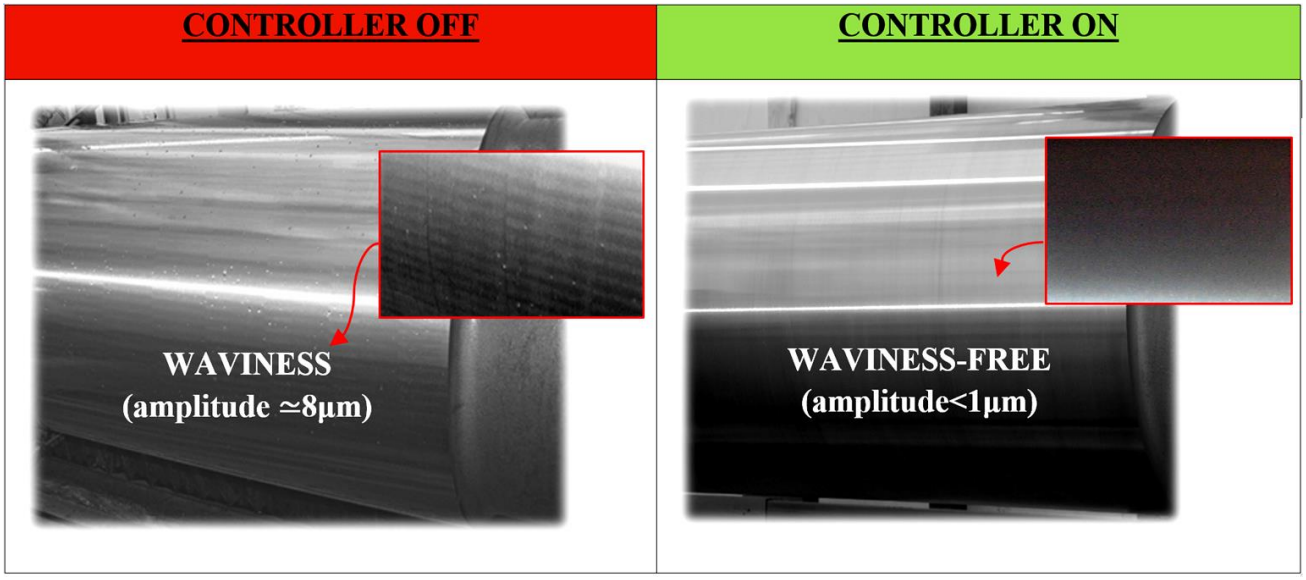

Figure 14: Workpiece surface finish after the application of the controller (Test ID6).

Cutting Test n°1	*Cutting Test n°2*	*Cutting Test n°3*
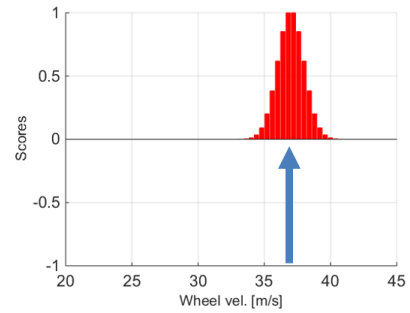	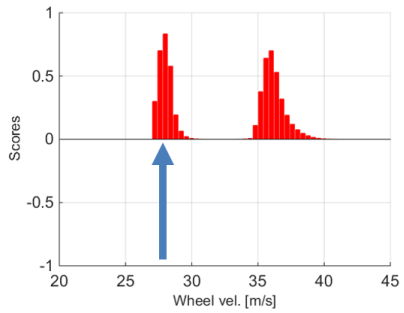	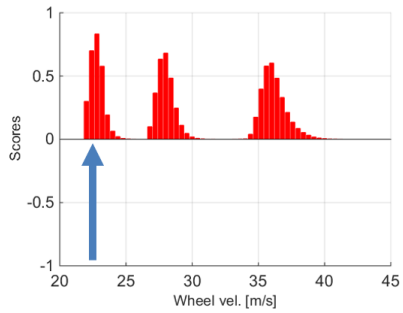
Stable speed =35.91 m/s	**Stable speed =27.93 m/s**	**Stable speed =22.88 m/s**
Positive score assigned to neighbor velocity bins	Positive score assigned to neighbor velocity bins	Positive score assigned to neighbor velocity bins
Cutting Test n°4	***Cutting Test n°5***	***Cutting Test n°8***
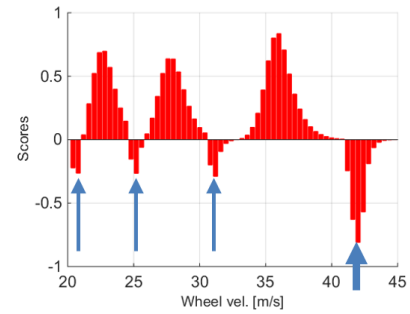	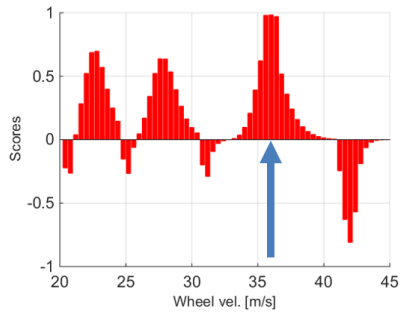	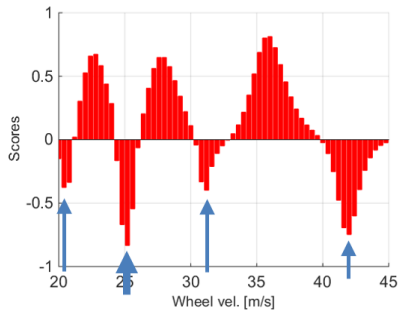
Unstable speed =41,89 m/s	**Stable speed =35.91 m/s**	**Unstable speed =25,17 m/s**
High negative scores assigned to neighbor velocity bins and lower negative score to their sub-harmonics	Positive score confirmed to neighbor velocity bins	High negative scores assigned to neighbor velocity bins and lower negative scores confirmed to their harmonics and sub-harmonics.

Figure 15. Learning tests of the machine Stability Map: (cutting tests n°1-2-3-4-5-8)

4. DISCUSSION AND CONCLUSION

The current manufacturing environment places a growing demand on control of unattended manufacturing processes and machines or automatic advice to unexperienced operators. This paper discusses the design and the performance of an automatic process controller for traverse grinding, focusing on reduction of the waviness caused by chatter vibration on the machined surface. This objective has been addressed with different model-based monitoring and mitigation techniques for wheel regenerative chatter that was revealed the main issue to tackle during roughing and semi-finishing operation in big industrial roll grinding machines.

The assessment of process controller performance has been carried out by experiments on an industrial roll grinder. Good performance have been achieved mainly by adopting spindle speed tuning, showing that workpiece waviness can be avoided while maintaining the productivity of the machine almost unvaried, namely, without changing passes overlap and/or cylinder velocity. The controller integrates also the continuous Spindle Speed Variation, as an alternative vibration mitigation method, that extends the chatter control functionalities. Further research can be devoted to verify the effectiveness of the continuous speed variation method both for wheel and workpiece chatter. For monitoring chatter onset, the controller exploits accelerometers but additional sensors could be adopted for integrating this diagnostic capability. For instance, the large and extended sensitivity in detecting the process perturbation provided by the AE sensors, usually installed on grinders as "contact-detection sensors", can be integrated in the chatter indicators by simply adding this sensor in the computation. Since, in the test machine, the accelerometers provided sufficient results the AE sensors have not been taken into account, and will be considered in future developments.

In order to maximize both effectiveness and robustness, the proposed "grey-box/model-based" solutions have been merged, with a "black-box/feed-back" approach that realizes a pure adaptive controller. The main innovation provided by this study consists in the automatic choice of the most stable wheel speed. Speed tuning actions are based on an adaptive Stability Map that evolves according to the experimental evidence of stability and instability of the cutting conditions. The map could be initialized with the theoretical stability lobes diagram calculated starting from a proper set of Frequency Response Function measurements and process coefficients, but skipping this phase does not produce a significant reduction of the overall performance. In fact, it has been demonstrated that the controller is capable of synthesizing in an automatic way the stability map for an industrial machine and that this information can be effectively transformed by the control logic in surface quality improvement in the final workpieces.

The controller, can be improved by including further diagnostic features, to manage machine anomalies that can hinder the controller actions, in order to support the industrial exploitability of the solution. Additionally, speed tuning actions will have to take into account not only stability of the cutting process, but also additional technological constraints and merit factors such as surface roughness and optical appearance or the overall system productivity and costs. Thanks to the flexibility of the design, the controller can be adapted also to work with different grinding machines.

5. ACKNOWLEDGMENTS

This work has been supported by funding of the Italian Ministry of Economic Development under the research program Industria 2015 "Michelangelo" (D.M. n. 00052MIOl).

6. REFERENCES

[1] Panjkovic V, Gloss R, Steward J, Dilks S, Steward R, Fraser G, Causes of chatter in a hot strip mill: Observations, qualitative analyses and mathematical modelling. J Mater Process Tech 2012; 212(4):954-961.

[2] Rowe WB, Li Y, Mills B, Allanson DR, Application of intelligent CNC in grinding. Computers in Industry 1996; 31(1):45-60.

[3] Chen T, Tian X, An intelligent self-learning method for dimensional error pre-compensation in CNC grinding. Int J Adv Manuf Technol 2014; 75:1349-1356.

[4] Choi HS, Lee SK, Machining error compensation of external cylindrical grinding using thermally actuated rest. Mechatronics 2002; 12(5):643-656

[5] Möhring HC, Gümmer O, Fischer R, Active error compensation in contour-controlled grinding. CIRP Annals - Manufacturing Technology 2011; 60(1):429-432

[6] Hekman KA, Liang, SY, Flatness control in grinding by depth of cut manipulation. Mechatronics 1998; 8:323-335

[7] Inasaki I, Sensor Fusion for Monitoring and Controlling Grinding Processes. Int J Adv Manuf Technol 1999; 15(10):730-736.

[8] Yuan L, Järvenpää VM, Keskinen E, Design of Fuzzy Logic-Based Controller in Roll Grinding System With Double Regenerative Chatter. Report from Laboratory of Machine Dynamics, Tampere University 2004.

[9] Oh CJ, Kim OH, A Study on Enhancement of Grinding Accuracy by an Active Tool Control. KSME International Journal 2002; 16(5):633-638.

[10] Albizuri J, Fernandes MH, Garitaonandia I, Sabalza X, Uribe-Etxeberria R, Hernández JM, An active system of reduction of vibrations in a centerless grinding machine using piezoelectric actuators. Int J Mach Tools Manuf 2007; 47(10):1607-1614.

[11] Nakano Y, Kato H. Tobita T, Uetake A, Uno M, Suppression Of Chatter Marks In Surface Grinding By Using Dynamic Damper. B Jpn Soc Prec Eng 1988; 22(1):37-42.

[12] Altintas Y, Weck M, Chatter stability of metal cutting and grinding. CIRP Ann-Manuf Techn 2004; 53:619-42.

[13] Inasaki I, Karpuschewski B, Lee HS, Grinding-Chatter Origin and suppression. CIRP Ann-Manuf Techn 2001; 50(2): 515-534.

[14] Thompson RA, Methods and apparatus for optimizing grinding. United States Patent, US4604834A, 1986.

[15] Thompson RA, On the doubly regenerative stability of a grinder: The mathematical analysis of chatter growth. ASME J. Eng. Ind. Ser. B 1986; 108(2):83–92.

[16] Orynski F, Pawlowski W, The mathematical description of dynamics of the cylindrical grinder. Int J Mach Tools Manuf 2002: 42:773-780.

[17] Li H, Shin YC, A study on chatter boundaries of cylindrical plunge grinding with process condition-dependent dynamics. Int J Mach Tools Manuf 2006; 47:1563-1572.

[18] Alvarez J, Barrenetxea D, Marquinez JI, Bediaga I, Gallego I, Effectiveness of continuous workpiece speed variation (CWSV) for chatter avoidance in throughfeed centerless grinding. Int J Mach Tools Manuf 2011; 51:911-917.

[19] Pearce T, The effect of continuous dressing on the occurrence of chatter in cylindrical grinding. Int J Mach Tool Manuf 1984; 24(2):77-86.

[20] Leonesio M, Parenti P, Cassinari A, Bianchi G, Force-field instability in surface grinding. Int J Adv Manuf Technol 2014; 72(9):1347-1360.

[21] Mannan M, Fan WT, Stone BJ, The effects of torsional vibration on chatter in grinding. J Mater Process Tech 1999; 90:303-309.

[22] Baylis R, Stone B, The effect of grinding wheel flexibility on chatter. CIRP Ann-Manuf Techn 1989; 38(1):307-310.

[23] Tönshoff H K, Friemuth T, Becker JC, Process monitoring in grinding. CIRP Ann-Manuf Techn 2002; 51(2):551-571.

[24] Fu JC, Troy CA, Mori K, Chatter classification by entropy functions and morphological processing in cylindrical traverse grinding. Precis Eng 1996; 18:110-117.

[25] González-Brambila O, Rubio E, Jáuregui JC, Herrera-Ruiz G, Chattering detection in cylindrical grinding processes using the wavelet transform. Int J Mach Tools Manuf 2006; 46:1934-1938.

[26] Sakarovitch J, Elements of automata theory. Translated from the French by Reuben Thomas. Cambridge University Press, 2009, ISBN 978-0-521-84425-3.

[27] Marinescu I, Hitchiner M, Uhlmann E, Rowe WB, Inasaki I, Handbook of Machining with Grinding Wheels. London: CRC Press; 2006. Chapter 2/4/8.

[28] Van Dijk M, Doppenberg EJJ, Faassen RPH, Van de Wouw N, Automatic In-Process Chatter Avoidance in the High-Speed Milling Process. J Dyn Syst-T Asme 2010; 132:031006-1.

[29] Parenti P, Leonesio M, Cassinari A, Bianchi G, Monno M, A model-based approach for online estimation of surface waviness in roll grinding. Int J Adv Manuf Technol 2015; 79(5):1195-1208.

[30] Geometrical product specifications (GPS) -- Roundness -- Part 1: Vocabulary and parameters of roundness, ISO 12181-1:2011. Geneva, Switzerland: ISO.